
Article:
Chan, H.-F. orcid.org/0000-0002-5382-2097, Weatherley, N., Johns, C. et al. (4 more authors) (2019) Airway microstructure in idiopathic pulmonary fibrosis: assessment at hyperpolarized 3He diffusion-weighted MRI. Radiology. ISSN 0033-8419

https://doi.org/10.1148/radiol.2019181714

Radiology

ORIGINAL RESEARCH • THORACIC IMAGING

Airway Microstructure in Idiopathic Pulmonary Fibrosis: Assessment at Hyperpolarized ^{3}He Diffusion-weighted MRI

Ho-Fung Chan, PhD • Nicholas D. Weatherley, BMSc* • Christopher S. Johns, PhD • Neil J. Stewart, PhD • Guilhem J. Collier, PhD • Stephen M. Bianchi, PhD • Jim M. Wild, PhD*

From the POLARIS, Academic Unit of Radiology, Infection, Immunity and Cardiovascular Disease, University of Sheffield, C Floor, Royal Hallamshire Hospital, Glossop Rd, Sheffield, S10 2JF, England (H.F.C., N.D.W., C.S.J., N.J.S., G.J.C., J.M.W.); Academic Directorate of Respiratory Medicine, Sheffield Teaching Hospitals NHS Foundation Trust, Sheffield, England (N.D.W., S.M.B.); and Department of Radiology, Sheffield Teaching Hospitals NHS Foundation Trust, Sheffield, England (C.S.J.). Received July 23, 2018; revision requested September 19; revision received November 16; accepted January 2, 2019. **Address correspondence to** J.M.W. (e-mail: *j.m.wild@sheffield.ac.uk*).

Study supported by National Institute for Health Research (NIHR-RP-R3-12-027) and the Medical Research Council (MR/M008894/1). The views expressed in this publication are those of the authors and not necessarily those of the National Health Service, the National Institute for Health Research or the Department of Health.

*H.F.C. and N.D.W. contributed equally to this work.

Conflicts of interest are listed at the end of this article.

See also the editorial by Altes and Flors in this issue.

Radiology 2019; 00:1–7 • https://doi.org/10.1148/radiol.2019181714 • Content code: CH

Background: MRI with inhaled hyperpolarized helium 3 (^{3}He) allows for functional and structural imaging of the lungs. Hyperpolarized gas diffusion-weighted (DW) MRI provides noninvasive and quantitative assessment of microstructural acinar changes in the lungs.

Purpose: To investigate whether microstructural imaging metrics from in-vivo hyperpolarized ^{3}He DW MRI are sensitive to longitudinal changes in a cohort of participants with idiopathic pulmonary fibrosis (IPF) and to evaluate the reproducibility of these metrics and their correlation with existing clinical measures of IPF disease severity.

Materials and Methods: In this prospective study, 18 participants with IPF underwent ^{3}He DW MRI at 1.5 T and 11 participants underwent an identical same-day examination for reproducibility assessment. Thirteen participants returned for 6- and 12-month follow-up examinations. Pulmonary function tests, including diffusing capacity of the lungs for carbon monoxide and forced vital capacity, were performed at each examination. The apparent diffusion coefficient (ADC) and stretched exponential model–derived mean diffusive length scale (Lm_D) from DW MRI was compared with baseline CT fibrosis scores and pulmonary function tests by using Spearman rank correlation coefficient. Longitudinal changes in DW MRI and pulmonary function test measurements were assessed with Friedman tests and post hoc Dunn test.

Results: ^{3}He ADC and Lm_D were reproducible (mean Bland-Altman analysis bias, 0.002 $cm^2 \cdot sec^{-1}$ and −1.5 μm, respectively). Elevated ADC and Lm_D regions qualitatively corresponded to fibrotic regions at CT. ADC and Lm_D correlated with diffusing capacity of the lungs for carbon monoxide (respectively: $r = -0.56$, $P = .017$; and $r = -0.54$, $P = .02$) and CT fibrosis score (respectively: $r = 0.71$, $P = .001$; and $r = 0.65$, $P = .003$). Lm_D increased by 12 μm after 12 months ($P = .001$) whereas mean ADC ($P = .17$), forced vital capacity ($P = .12$), and diffusing capacity of the lungs for carbon monoxide ($P > .99$) were not statistically different between examinations.

Conclusion: Helium 3 diffusion-weighted MRI-derived mean diffusive length scale demonstrates longitudinal changes in lungs affected by idiopathic pulmonary fibrosis.

Online supplemental material is available for this article.

Idiopathic pulmonary fibrosis (IPF) is a progressive and usually fatal lung disease that occurs in the 6th and 7th decades of life (1). This group of diseases is defined by the lack of an underlying cause and the presence of usual interstitial pneumonia, typically identified at CT with honeycombing, reticulation, and traction bronchiectasis (2). Usual interstitial pneumonia is spatially heterogeneous, both macroscopically and microscopically, demonstrating a peripheral and basal predominant distribution. Despite recently available therapies that appear to slow the rate of disease progression (3,4), current measures of disease severity are insensitive and nonspecific, prompting searches for clinical and imaging biomarkers of disease to assist with phenotyping, prognostication, and the development of therapies (5,6).

MRI with inhaled hyperpolarized helium 3 (^{3}He) or xenon 129 (^{129}Xe) allows for functional and structural imaging of the lungs (7,8). Hyperpolarized gas diffusion-weighted (DW) MRI enables noninvasive and quantitative assessment of microstructural acinar changes (9,10). The derived apparent diffusion coefficient (ADC) and lung morphometry parameters from theoretical gas diffusion models correlate with diffusing capacity of the lungs for carbon monoxide and carbon monoxide transfer coefficient in diseases characterized by a loss of alveolar integrity,

Abbreviations

ADC = apparent diffusion coefficient, DW = diffusion weighted , IPF = idiopathic pulmonary fibrosis, Lm_D = mean diffusive length scale

Summary

Hyperpolarized helium 3 diffusion-weighted MRI metrics were elevated in lungs with idiopathic pulmonary fibrosis, and diffusion model estimates of airway mean diffusive length scale demonstrated sensitivity to longitudinal change.

Key Points

- The apparent diffusion coefficient (ADC) and stretched exponential model derived mean diffusive length scale (Lm_D) from diffusion-weighted MRI were reproducible (mean Bland-Altman analysis bias, 0.002 $cm^2 \cdot sec^{-1}$ and −1.5 μm, respectively).
- Regions with elevated ADC and Lm_D qualitatively corresponded to fibrotic regions at CT.
- Lm_D increased by 12 μm after 12 months ($P = .001$) whereas the mean ADC ($P = .17$), forced vital capacity ($P = .12$), and diffusing capacity of the lungs for carbon monoxide ($P > .99$) were not statistically different between examinations.

such as the emphysematous component of chronic obstructive pulmonary disease (11,12).

Previous ^{3}He and ^{129}Xe DW MRI studies of IPF have been predominantly restricted to the imaging of explanted lungs affected by IPF (13,14) in which affected lungs were used as control specimens and compared with lungs affected by chronic obstructive pulmonary disease. Initial in vivo ^{3}He DW MRI in fibrotic lungs demonstrated elevated ADC values (15), but to our knowledge, no longitudinal studies in individuals with IPF have been reported.

The purpose of our study was to investigate whether in vivo hyperpolarized ^{3}He DW MRI metrics are sensitive to longitudinal changes in a cohort of individuals with IPF. In addition, we evaluated the reproducibility of these microstructural imaging metrics and their correlation with existing clinical measures of IPF disease severity.

Materials and Methods

This prospective study from February 2016 to February 2018 was approved by the Liverpool Central National Health Service Research Ethics Committee. Written consent was obtained from each participant.

Study Participants

Eighteen participants (15 men and three women; mean age, 71.4 years ± 5.5 [standard deviation]; age range, 61–80 years) who were diagnosed with IPF were recruited by a multidisciplinary team at a single tertiary center for interstitial lung disease. Participants were imaged at baseline, and 13 of the participants returned for follow-up examinations after 6 and 12 months for longitudinal assessment. Four participants died between follow-up examinations, and one participant was too sick to return for sequential study examinations.

MRI and Analysis

All 18 participants underwent hyperpolarized ^{3}He DW MRI at baseline, and 11 participants underwent a second identical same-day examination for reproducibility assessment. Participants were repositioned approximately 15 minutes after baseline examination for the same-day repeat examination. ^{3}He DW MRI was performed on a 1.5-T imager (GE HDx; GE Healthcare, Milwaukee, Wis) by using a quadrature chest radiofrequency coil (Clinical MR Solutions, Brookfield, Wis) with a three-dimensional multiple b value spoiled gradient–echo sequence with compressed sensing undersampling (16). Four DW interleaved acquisitions (b values: 0, 1.6, 4.2, and 7.2 sec/cm^2; diffusion time, 1.6 msec) were acquired during a single 15-second breath-hold examination after the inhalation of a 1-L gas mixture from functional residual capacity consisting of 250 mL of hyperpolarized ^{3}He (~25% polarization) and 750 mL of nitrogen. Participants were coached by a lung physiologist to achieve functional residual capacity and practiced inhaling 1 L of room air before undergoing imaging.

All MR image analyses were performed by one author (H.F.C., with 4 years of experience analyzing ^{3}He DW MRI) using in-house software code (Matlab R2017a; Mathworks, Natick, Mass). ADC and mean diffusive length scale (Lm_D) values were calculated for each data set on a voxel-by-voxel basis. ADC was derived from a monoexponential fit of signal intensities of the first two DW interleaves (b = 0 and b = 1.6 sec/cm^2). The stretched exponential function was used to fit the signal intensities of all four DW interleaved acquisitions to derive a Lm_D value, an estimate of mean alveolar dimension; full details are described in Chan et al (16). Global mean values of ADC and Lm_D for each data set were obtained from the average of all ADC and Lm_D values within the lung.

Pulmonary Function Tests

Same-day pulmonary function tests were performed during each examination, including forced vital capacity, diffusing capacity of the lungs for carbon monoxide, and carbon monoxide transfer coefficient. Percentage predicted values for age and sex were calculated by using the Global Lung Initiative reference values (17).

CT Imaging and Analysis

Multi–detector row CT of the thorax was performed as close as was practical to the baseline MRI (mean, 55.7 days ± 61.7). Sixteen participants underwent noncontrast multi–detector row CT at one tertiary center on a 64-section scanner (Light-Speed; GE Medical) during a single full inspiration breath hold; the remaining two participants underwent multi–detector row CT at a separate referring hospital. CT images were reconstructed to 1.25-mm-thick sections, and the mean dose-length product for all participants was 313 mGy · cm (range, 101–743 mGy · cm).

CT images were visually assessed for interstitial lung disease severity by using a semiquantitative Likert scoring scale (18) by a single trained thoracic radiologist (C.S.J., with 6 years of experience) who was blinded to all clinical information. Each lobe, considering the lingula as a lobe, was scored from 0 to 4 (0, no fibrosis; 1, 1%–25% fibrosis; 2, 26%–50% fibrosis; 3, 51%–75% fibrosis; and 4, 76%–100% fibrosis).

Table 1: Participant Demographics, Baseline, and Same-Day Repeat Baseline Metrics from Pulmonary Function Tests, ^{3}He Diffusion-weighted MRI, and CT Imaging

Parameter	Baseline	Same-Day Baseline Repeat
No. of participants	18	11
Age (y)	71.4 ± 5.5	70.8 ± 5.5
Sex		
No. of men	15	9
No. of women	3	2
FVC (% predicted)	80.3 ± 17.4	84.5 ± 20.3
D_{LCO} (% predicted)	46.7 ± 18.8	50.9 ± 18.9
K_{CO} (% predicted)	72.6 ± 21.2	68.6 ± 14.4
^{3}He SNR	23 ± 9	21 ± 9
Baseline repeat ^{3}He SNR	…	20 ± 7
^{3}He ADC ($cm^2 \cdot sec^{-1}$)	0.33 ± 0.07	0.32 ± 0.06
Baseline repeat ^{3}He ADC ($cm^2 \cdot sec^{-1}$)	…	0.32 ± 0.05
^{3}He Lm_D (μm)	272 ± 22	266 ± 16
Baseline repeat ^{3}He Lm_D (μm)	…	268 ± 13
Likert CT fibrosis score	10.2 ± 5.3	…

Note.—Data are mean ± standard deviation unless otherwise indicated. Helium 3 (^{3}He) signal-to-noise ratio (SNR) was calculated from the diffusion interleave without diffusion weighting (b = 0 sec/cm^2) and is corrected for Rician distribution bias. The Likert CT fibrosis score is a range of 0–24. ADC = apparent diffusion coefficient, D_{LCO} = diffused capacity of the lungs for carbon monoxide, FVC = forced vital capacity, K_{CO} = carbon monoxide transfer coefficient, Lm_D = mean diffusive length scale.

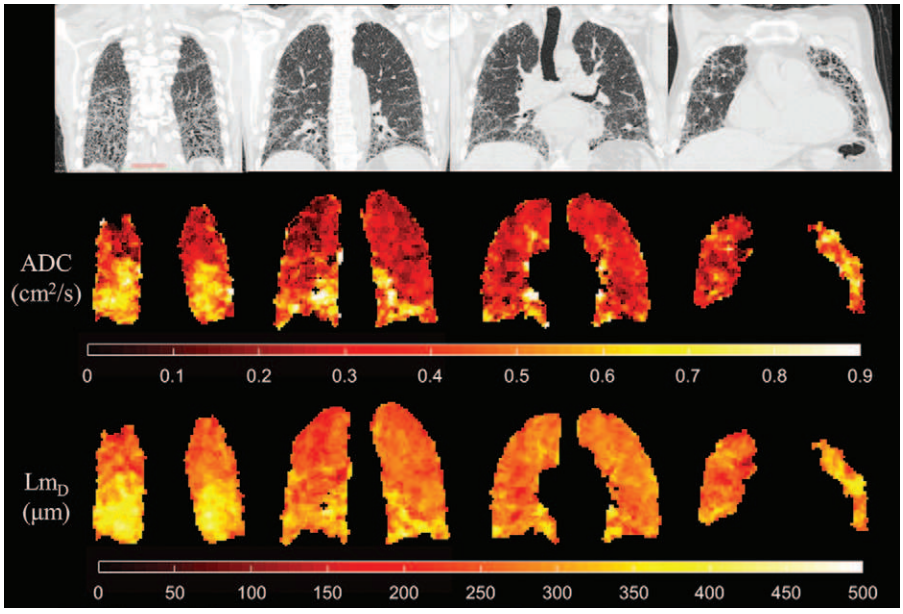

Figure 1: CT images and helum 3 (^{3}He) diffusion-weighted MR images acquired at baseline in a 74-year-old male study participant with idiopathic pulmonary fibrosis. Coronal CT images (top; section thickness, 1.25 mm) show fibrotic regions of the lung. Corresponding coronal ^{3}He apparent diffusion coefficient (ADC) and mean diffusive length scale (Lm_D) maps (middle and bottom; section thickness,12 mm) show areas of elevated values that are spatially correlated to the fibrotic regions at CT.

The score for each lung lobe was summed to provide a fibrosis score (out of 24) for the whole lung.

Statistical Analysis

Spearman rank correlation coefficient determined strength of correlation between pulmonary function tests and imaging metrics. Reproducibility of DW MRI metrics was assessed by using Bland-Altman analysis. Longitudinal differences in DW MRI and pulmonary function test measurements were assessed with Friedman tests and post hoc Dunn tests. All statistical analyses were performed by using software (SPSS version 23.0, IBM, Armonk, NY; and Prism version 7.04, GraphPad, La Jolla, Calif), and a P value of less than .05 indicated statistical significance.

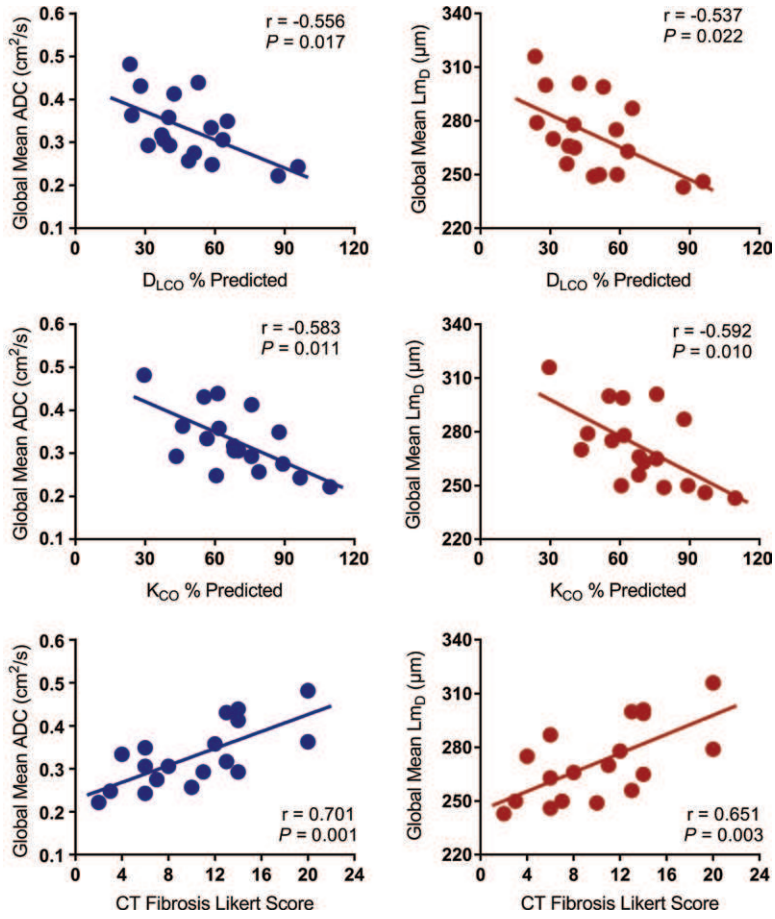

Figure 2: Scatter plots demonstrate the relationship between helium 3 diffusion-weighted MRI–derived apparent diffusion coefficient (ADC) and mean diffusive length scale (Lm_D) values, and percentage predicted (% predicted) diffused capacity of the lungs for carbon monoxide (D_{LCO}), carbon monoxide transfer coefficient (K_{CO}), and semiquantitative CT fibrosis Likert score. Both global mean ADC and Lm_D values show linear correlations with percentage predicted D_{LCO}, K_{CO}, and CT fibrosis Likert score.

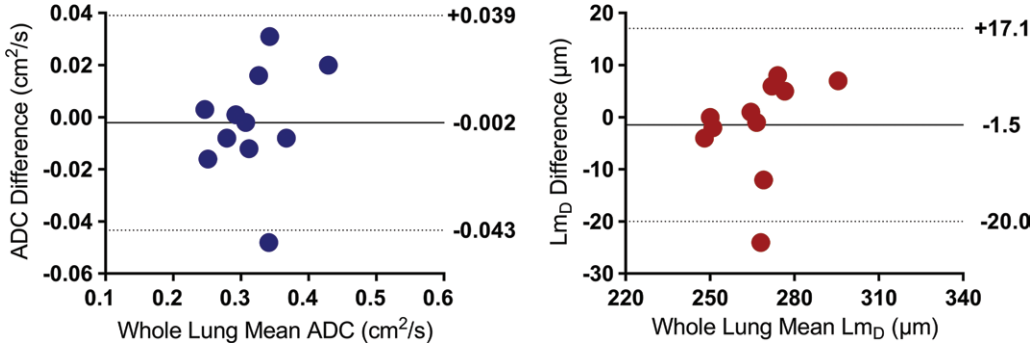

Figure 3: Bland-Altman comparison of global mean apparent diffusion coefficient (ADC) and mean diffusive length scale (Lm_D) values for 11 participants with idiopathic pulmonary fibrosis (IPF) who underwent both imaging at baseline and same-day repeat baseline examinations.

Results

Baseline and Reproducibility Results

A summary of participant demographics and baseline measurements for our cohort of participants with IPF are shown in Table 1 and Table E1 (online). The global mean ^3He ADC and Lm_D values for this cohort were 0.33 $cm^2 \cdot sec^{-2}$ ± 0.07 and 272 µm ± 22, respectively. Regions of relatively high ADC and elevated Lm_D values appear to spatially correlate with fibrotic regions on the accompanying CT sections (Fig 1). Both percentage predicted carbon monoxide transfer coefficient and diffusing capacity of the lungs for carbon

Table 2: Summary of Pulmonary Function Tests and ^{3}He Diffusion-weighted MRI Metrics in Study Participants with Idiopathic Pulmonary Fibrosis

Parameter	Baseline	6-month Examination	12-month Examination	Friedman Test *P* Value
FVC (% predicted)	83.9 ± 18.7	80.2 ± 18.9	79.9 ± 19.5	.12
D_{LCO} (% predicted)	58.3 ± 18.1	57.8 ± 19.7	58.2 ± 20.6	.9
K_{CO} (% predicted)	76.4 ± 16.5	75.3 ± 15.8	75.4 ± 16.6	.34
^{3}He SNR (b = 0 sec/cm^2)	23 ± 11	32 ± 13	37 ± 11	.009
^{3}He ADC (cm^2 · sec^{-1})	0.31 ± 0.07	0.32 ± 0.06	0.32 ± 0.07	.17
^{3}He Lm_D (μm)	266 ± 20	275 ± 21	279 ± 24	.002

Note.—Data are mean ± standard deviation. Thirteen study participants were included; however, longitudinal diffused capacity of the lungs for carbon monoxide and carbon monoxide transfer coefficient tests were available in 12 study participants only. ^{3}He = helium 3, ADC = apparent diffusion coefficient, D_{LCO} = diffused capacity of the lungs for carbon monoxide, FVC = forced vital capacity, K_{CO} = carbon monoxide transfer coefficient, Lm_D = mean diffusive length scale, SNR = signal-to-noise ratio.

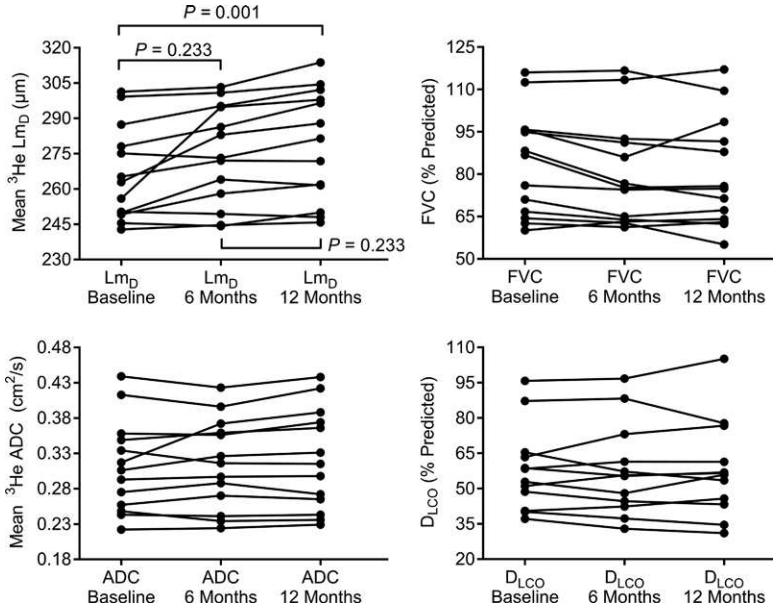

Figure 4: Point-to-point plots of global mean diffusive length scale (Lm_D), mean apparent diffusion coefficient (ADC), forced vital capacity (FVC), and diffused capacity of the lungs for carbon monoxide (D_{LCO}) for baseline and 6- and 12-month follow-up examinations in 13 participants with IPF.

monoxide were correlated with mean ADC (respectively: r = −0.58, P = .01; and r = −0.56, P = .02) and Lm_D (respectively: r = −0.59, P = .01; and r = −0.54, P = .02, respectively) (Fig 2). Forced vital capacity percentage predicted was not correlated with either the mean ADC (P = .65) or Lm_D (P = .75) value. The average CT fibrosis (ie, Likert) score was 10 ± 5 of 24 and correlated with global mean ^{3}He ADC (r = 0.70; P = .001) and Lm_D (r = 0.65; P = .003) values (Fig 2).

Same-day mean ADC and Lm_D values in the 11 participants with IPF assessed at baseline were reproducible. Mean ADC for baseline examination 1 and baseline examination 2 was 0.32 cm^2 · sec^{-2} ± 0.06 and 0.32 cm^2 · sec^{-2} ± 0.05, respectively. Lm_D for baseline examination 1 and baseline examination 2 was 266 μm ± 16 and 268 μm ± 13, respectively. Bland-Altman analysis of global mean ADC and Lm_D values between both baseline examinations resulted in a mean ADC bias of −0.002 cm^2 · sec^{-2} (95% confidence interval: −0.043 cm^2 · sec^{-2}, 0.039 cm^2 · sec^{-2}; mean percentage bias, −0.9%; 95% confidence interval: −13.1%, 11.3%) and a mean Lm_D bias of −1.5 μm (95% confidence interval: −20.0 μm, 17.1 μm; mean percentage bias, −0.6%; 95% confidence interval: −7.4%, 6.3%; Fig 3).

Longitudinal Results

Table 2 and Table E2 (online) summarize the longitudinal assessment of DW MRI and pulmonary function test metrics in participants with IPF. A trend toward increased mean ^{3}He ADC and Lm_D and decreased forced vital capacity was observed over 6 and 12 months. Friedman tests determined that Lm_D was different between examinations (χ^2 = 12.46; P = .002), whereas ADC (P = .17), forced vital capacity (P = .12), diffusing capacity of the lungs for carbon monoxide (P > .99), and carbon monoxide transfer

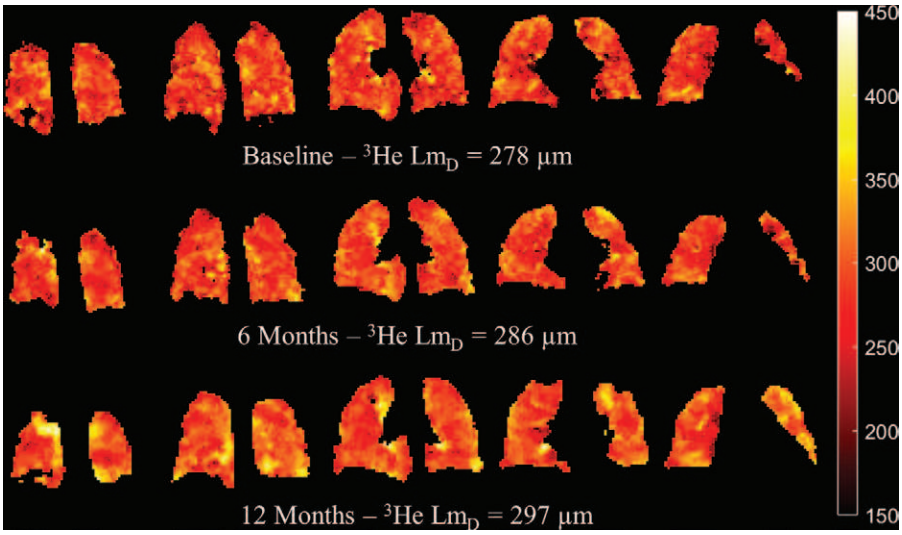

Figure 5: Selected coronal helium 3 (^{3}He) mean diffusive length scale (Lm_D) maps for a 71-year-old male study participant with idiopathic pulmonary fibrosis who exhibited a 19-μm increase in Lm_D after 12 months. Global Lm_D value increased between each examination and was characterized by a higher number of elevated Lm_D regions, typically in the basal and peripheral regions of the lungs.

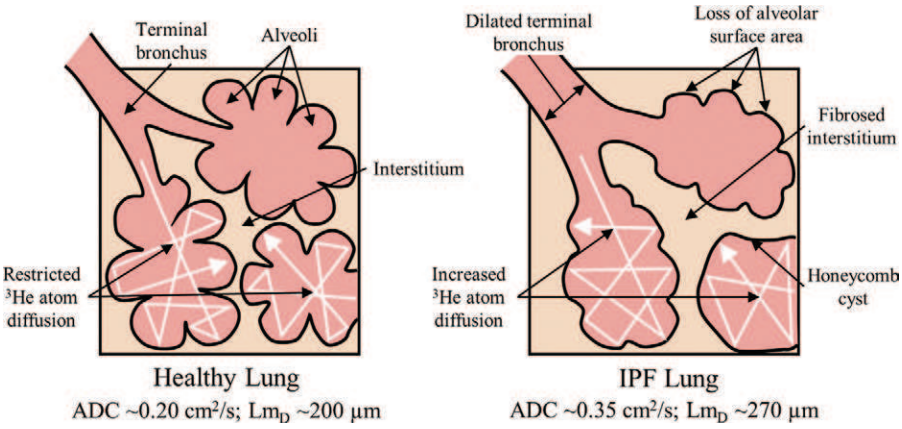

Figure 6: Schematic of helium 3 (^{3}He) gas atom diffusion (white arrows) in a healthy lung and a lung with idiopathic pulmonary fibrosis (IPF). Healthy alveolar structures restrict ^{3}He diffusion in the healthy lung. However, in the IPF lung, fibrotic changes lead to a loss of alveolar surface area, the formation of honeycomb cysts, and dilation of terminal bronchi. These factors all contribute to higher ^{3}He diffusion and elevated apparent diffusion coefficient (ADC) and mean diffusive length scale (Lm_D) values from healthy participants (16).

coefficient (P = .34) were not statistically different (Fig 4). Post hoc Dunn tests conducted for Lm_D value determined an increase of 12.4 μm in global Lm_D value between baseline and 12 months (P = .001). However, no difference was observed between examinations at baseline and 6 months (P = .22), and 6 months and 12 months (P = .23). Example Lm_D maps corresponding to a participant with IPF in which an increase in mean global Lm_D was observed are shown in Figure 5, on which more elevated Lm_D regions are observed in the basal and peripheral regions of the selected coronal maps over time.

Discussion

In our cohort of participants with IPF, the mean ^{3}He ADC and Lm_D derived by using DW MRI are elevated compared with reported values in young and older healthy patients acquired with the same b value and inflation state at 1.5 T (16,19) and 3.0 T (20,21). ^{3}He DW MRI metrics were reproducible in lungs affected by IPF; same-day variability was similar to that reported previously for ADC (19) and lung morphometry parameters (22) in healthy participants and patients with chronic obstructive pulmonary disease. Elevated ADC, which is reflective of higher Brownian gas diffusion in the acinar airways, is consistent with the results obtained from explanted and in vivo lungs with fibrosis (13,15), but is different than the decreased ADC observed in rats induced with bleomycin models of drug-induced interstitial lung disease (23). This discrepancy may be because of pathologic and physiologic differences between IPF, an insidious pauci-immune idiopathic disease predominantly characterized by fibrosis, and the bleomycin animal model that is initially characterized by inflammation after a drug-induced organizing pneumonia.

We hypothesized that the elevated ADC and Lm_D values reflect loss of acinar integrity because of microstructural changes related to fibrosis (Fig 6). This is qualitatively substantiated by the elevated ADC and Lm_D typically evident in peripheral and basal regions on the DW MRI maps, congruous with the expected distribution of fibrotic disease at CT. The correlation with semiquantitative CT fibrosis score suggests sensitivity to honeycomb cysts and terminal bronchiolar dilation, characteristic of IPF lung disease. The correlations with carbon monoxide transfer coefficient and diffusing capacity of the lungs for carbon monoxide also suggests that the elevated DW MRI metrics are consistent with deteriorating alveolar gas transfer associated with the concomitant loss of alveolar surface area.

The absence of a significant decrease in forced vital capacity, diffusing capacity of the lungs for carbon monoxide, and carbon monoxide transfer coefficient during 12 months suggests that our cohort with IPF was clinically stable according to current clinical markers of IPF disease progression. However, a significant increase in global mean ^{3}He Lm_D value after 12 months was observed and corresponded to a larger number of elevated Lm_D regions typically in the base and periphery of Lm_D maps. This is consistent with the expected patterns of IPF progression and suggests that Lm_D from DW MRI may have greater sensitivity to progressive microstructural changes in lungs affected by

IPF compared with ADC or pulmonary function tests alone. Lm_D value may be useful as a quantitative metric for the assessment of early progressive microstructural changes in IPF that is hidden from the current clinical measures for disease progression that rely on pulmonary function tests.

Although it only visually showed a trend, the global mean ^{3}He ADC was not significantly different after 12 months. This discrepancy may be explained by the ADC monoexponential fit that does not account for the non-Gaussian diffusion observed in the lungs with hyperpolarized gas DW MRI (24). However, the multiple *b* value–stretched exponential fit to all DW data that is used to derive Lm_D fits the experimental measured diffusion signal decay more accurately (24), but we do not know whether the Lm_D values derived are consistent with alveolar dimensions observed at histologic analysis of IPF.

The primary limitation of our study was that in this small cohort of participants with IPF there were no other independent findings that corroborated our observed longitudinal change in Lm_D value. Longitudinal CT imaging after 12 months, in addition to assessment by a second radiologist, would further strengthen future comparative studies. Further work is required to corroborate whether the longitudinal microstructural changes observed at DW MRI coincide with structural changes observed at CT, and how these changes relate to discrete pathologic elements of IPF. Feasibility of three-dimensional whole-lung morphometry measurements derived from the cheaper and more abundant ^{129}Xe isotope was recently demonstrated (25) and is promising for the clinical viability of future longitudinal studies of IPF with DW MRI.

In conclusion, elevated apparent diffusion coefficient and mean diffusive length scale values, suggestive of terminal bronchiole and acinar airway enlargement, were observed in lungs with idiopathic pulmonary fibrosis by using in vivo hyperpolarized ^{3}He diffusion-weighted (DW) MRI. DW MRI metrics correlated with clinical measures of pulmonary gas exchange and CT fibrosis score. After 12 months, a significant increase in mean diffusive length scale value was demonstrated, whereas no difference in apparent diffusion coefficient value and pulmonary functions tests was observed.

Acknowledgments: The authors thank Laurie Smith, MS, and Matt Austin, BS, for help with lung function testing; Oliver Rodgers, Paul Hughes, PhD, Graham Norquay, PhD, and Madhwesha Rao, PhD for help polarizing gas for this study; Helen Marshall, PhD, Jody Bray, BS, and Dave Capener, MS, for assistance imaging; Leanne Armstrong and Jenny Rodgers, BA, with study coordination; and Steve Renshaw, PhD, for useful clinical discussions.

Author contributions: Guarantor of integrity of entire study, J.M.W.; study concepts/study design or data acquisition or data analysis/interpretation, all authors; manuscript drafting or manuscript revision for important intellectual content, all authors; approval of final version of submitted manuscript, all authors; agrees to ensure any questions related to the work are appropriately resolved, all authors; literature research, H.F.C., J.M.W.; clinical studies, N.D.W., C.S.J., G.J.C., J.M.W.; experimental studies, H.F.C., N.D.W., N.J.S., J.M.W.; statistical analysis, H.F.C., N.D.W., J.M.W.; and manuscript editing, all authors

Disclosures of Conflicts of Interest: **H.F.C.** disclosed no relevant relationships. **N.D.W.** disclosed no relevant relationships. **C.S.J.** disclosed no relevant relationships. **N.J.S.** disclosed no relevant relationships. **G.J.C.** disclosed no relevant relationships. **S.M.B.** Activities related to the present article: disclosed payments for expert panel attendance from Roche and Boehringer-Ingelheim. Activities not related to the present article: disclosed payments from Windsor Coroner for expert testimony; disclosed payment for speaker services from GlaxoSmithKline and Astra Zeneca; disclosed financial support from Boehringer for travel, accommodation, and entry fee costs related to European Respiratory Society London 2017. Other relationships: disclosed no relevant relationships. **J.M.W.** disclosed no relevant relationships.

References

1. Gross TJ, Hunninghake GW. Idiopathic pulmonary fibrosis. N Engl J Med 2001;345(7):517–525.
2. Raghu G, Collard HR, Egan JJ, et al. An official ATS/ERS/JRS/ALAT statement: idiopathic pulmonary fibrosis: evidence-based guidelines for diagnosis and management. Am J Respir Crit Care Med 2011;183(6):788–824.
3. Noble PW, Albera C, Bradford WZ, et al. Pirfenidone in patients with idiopathic pulmonary fibrosis (CAPACITY): two randomised trials. Lancet 2011;377(9779):1760–1769.
4. Richeldi L, du Bois RM, Raghu G, et al. Efficacy and safety of nintedanib in idiopathic pulmonary fibrosis. N Engl J Med 2014;370(22):2071–2082.
5. Maher TM. Disease stratification in idiopathic pulmonary fibrosis: the dawn of a new era? Eur Respir J 2014;43(5):1233–1236.
6. Maldonado F, Moua T, Rajagopalan S, et al. Automated quantification of radiological patterns predicts survival in idiopathic pulmonary fibrosis. Eur Respir J 2014;43(1):204–212.
7. MacFall JR, Charles HC, Black RD, et al. Human lung air spaces: potential for MR imaging with hyperpolarized He-3. Radiology 1996;200(2):553–558.
8. Mugler JP 3rd, Driehuys B, Brookeman JR, et al. MR imaging and spectroscopy using hyperpolarized 129Xe gas: preliminary human results. Magn Reson Med 1997;37(6):809–815.
9. Saam BT, Yablonskiy DA, Kodibagkar VD, et al. MR imaging of diffusion of (3)He gas in healthy and diseased lungs. Magn Reson Med 2000;44(2):174–179.
10. Kaushik SS, Cleveland ZI, Cofer GP, et al. Diffusion-weighted hyperpolarized 129Xe MRI in healthy volunteers and subjects with chronic obstructive pulmonary disease. Magn Reson Med 2011;65(4):1154–1165.
11. Fain SB, Panth SR, Evans MD, et al. Early emphysematous changes in asymptomatic smokers: detection with 3He MR imaging. Radiology 2006;239(3):875–883.
12. Paulin GA, Ouriadov A, Lessard E, Sheikh K, McCormack DG, Parraga G. Noninvasive quantification of alveolar morphometry in elderly never- and ex-smokers. Physiol Rep 2015;3(10):e12583.
13. Bink A, Hanisch G, Karg A, et al. Clinical aspects of the apparent diffusion coefficient in 3He MRI: results in healthy volunteers and patients after lung transplantation. J Magn Reson Imaging 2007;25(6):1152–1158.
14. Thomen RP, Quirk JD, Roach D, et al. Direct comparison of ^{129} Xe diffusion measurements with quantitative histology in human lungs. Magn Reson Med 2017;77(1):265–272.
15. Schreiber WG, Morbach AE, Stavngaard T, et al. Assessment of lung microstructure with magnetic resonance imaging of hyperpolarized Helium-3. Respir Physiol Neurobiol 2005;148(1-2):23–42.
16. Chan HF, Stewart NJ, Parra-Robles J, Collier GJ, Wild JM. Whole lung morphometry with 3D multiple b-value hyperpolarized gas MRI and compressed sensing. Magn Reson Med 2017;77(5):1916–1925.
17. Quanjer PH, Stanojevic S, Cole TJ, et al. Multi-ethnic reference values for spirometry for the 3-95-yr age range: the global lung function 2012 equations. Eur Respir J 2012;40(6):1324–1343.
18. Kim HG, Tashkin DP, Clements PJ, et al. A computer-aided diagnosis system for quantitative scoring of extent of lung fibrosis in scleroderma patients. Clin Exp Rheumatol 2010;28(5 Suppl 62):S26–S35.
19. Stewart NJ, Chan HF, Hughes PJC, et al. Comparison of ^{3} He and ^{129} Xe MRI for evaluation of lung microstructure and ventilation at 1.5T. J Magn Reson Imaging 2018;48(3):632–642.
20. Kirby M, Ouriadov A, Svenningsen S, et al. Hyperpolarized 3He and 129Xe magnetic resonance imaging apparent diffusion coefficients: physiological relevance in older never- and ex-smokers. Physiol Rep 2014;2(7):e12068.
21. Ouriadov A, Lessard E, Sheikh K, Parraga G; Canadian Respiratory Research Network. Pulmonary MRI morphometry modeling of airspace enlargement in chronic obstructive pulmonary disease and alpha-1 antitrypsin deficiency. Magn Reson Med 2018;79(1):439–448.
22. Quirk JD, Chang YV, Yablonskiy DA. In vivo lung morphometry with hyperpolarized (3) He diffusion MRI: reproducibility and the role of diffusion-sensitizing gradient direction. Magn Reson Med 2015;73(3):1252–1257.
23. Stephen MJ, Emami K, Woodburn JM, et al. Quantitative assessment of lung ventilation and microstructure in an animal model of idiopathic pulmonary fibrosis using hyperpolarized gas MRI. Acad Radiol 2010;17(11):1433–1443.
24. Parra-Robles J, Ajraoui S, Wild JM. Modelling non-Gaussian 3He diffusion signal behaviour using a fractional dynamics approach [abstr]. In: Proceedings of the Eighteenth Meeting of the International Society for Magnetic Resonance in Medicine. Berkeley, Calif: International Society for Magnetic Resonance in Medicine, 2010; 2538.
25. Chan HF, Stewart NJ, Norquay G, Collier GJ, Wild JM. 3D diffusion-weighted ^{129} Xe MRI for whole lung morphometry. Magn Reson Med 2018;79(6):2986–2995.